**Cell Reports, Volume *34***

## Supplemental information

# Omnitemporal choreographies of all five STIM/Orai and $IP_3Rs$ underlie the complexity of mammalian $Ca^{2+}$ signaling

**Scott M. Emrich, Ryan E. Yoast, Ping Xin, Vikas Arige, Larry E. Wagner, Nadine Hempel, Donald L. Gill, James Sneyd, David I. Yule, and Mohamed Trebak**

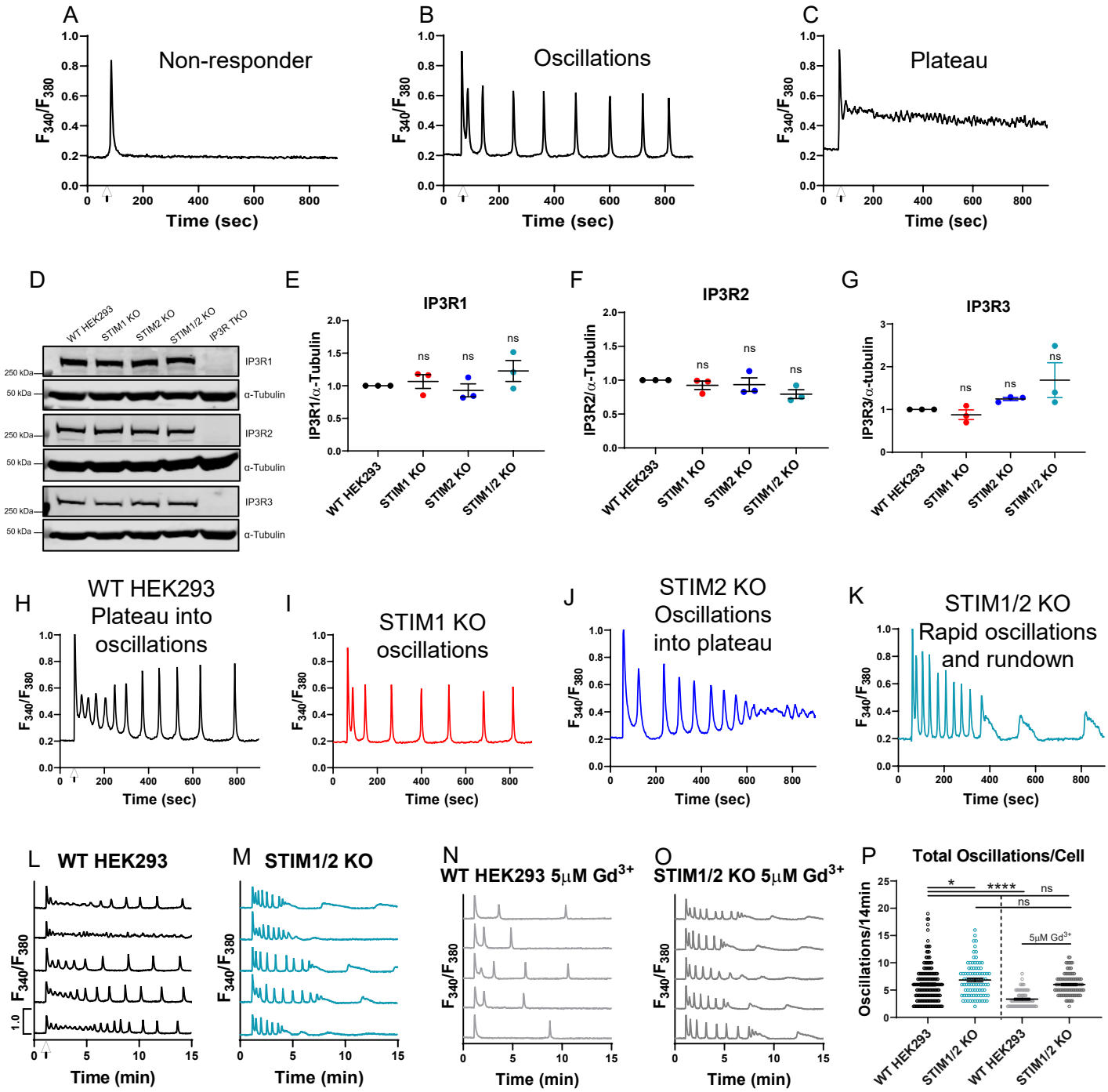


**Supplementary Figure 1. $IP_3R$ isoform expression, and effect of $Gd^{3+}$ on $Ca^{2+}$ oscillation profiles in WT HEK293 and STIM-KO cells (Related to Figure 1).** Traces representing the three oscillatory profiles quantified throughout the manuscript. (A) Non-responding cells demonstrate no response or a single initial spike that returns to baseline following agonist stimulation. (B) Cells showing regenerative oscillations that return to baseline prior to each subsequent spike for the duration of the recording. (C) Plateau cells with sustained elevation of cytosolic $Ca^{2+}$ for the duration of the recording. The arrow in each trace represents the time of addition of 10μM carbachol (CCh). (D) Western blot analysis of $IP_3R1/2/3$ isoforms in WT HEK293 and STIM knockout cell lines. (E) Quantification of $IP_3R1$ intensity normalized to α-tubulin loading control. Each point represents an individual biological replicate ($n$ = 3 each for each condition). (F) Quantification of $IP_3R2$ intensity ($n$ = 4 each for each condition). (G) Quantification of $IP_3R3$ intensity ($n$ = 3 each for each condition). (H) Characteristic $Ca^{2+}$ oscillation profiles in WT HEK293, (I) STIM1-KO, (J) STIM2-KO, and (K) STIM1/2-KO cell lines in response to 10μM CCh stimulation (represented by arrow in H). (L) $Ca^{2+}$ traces from 5 representative cells/condition upon stimulation with 10 μM carbachol (CCh) at 1 minute (indicated by arrow in L) in the presence of 2mM external $Ca^{2+}$. WT HEK293 cells were stimulated in the absence or (N) presence of 5μM $Gd^{3+}$. (M) Representative $Ca^{2+}$ traces of STIM1/2-KO cells in the absence or (O) presence of 5μM $Gd^{3+}$. (P) Quantification of total oscillations in 14 minutes from (L-O). From left to right $n$ = 189, 90, 78, and 113 individual cells. Scatter plot in (P) is presented as mean ± SEM and analyzed with the Kruskal-Wallis one-way ANOVA with multiple comparisons to WT HEK293 cells (*p<0.05; ****p<0.0001; ns, not significant). Comparison between STIM1/2-KO cells in the absence or presence of 5μM $Gd^{3+}$ was performed with the Mann-Whitney U test (ns, not significant).

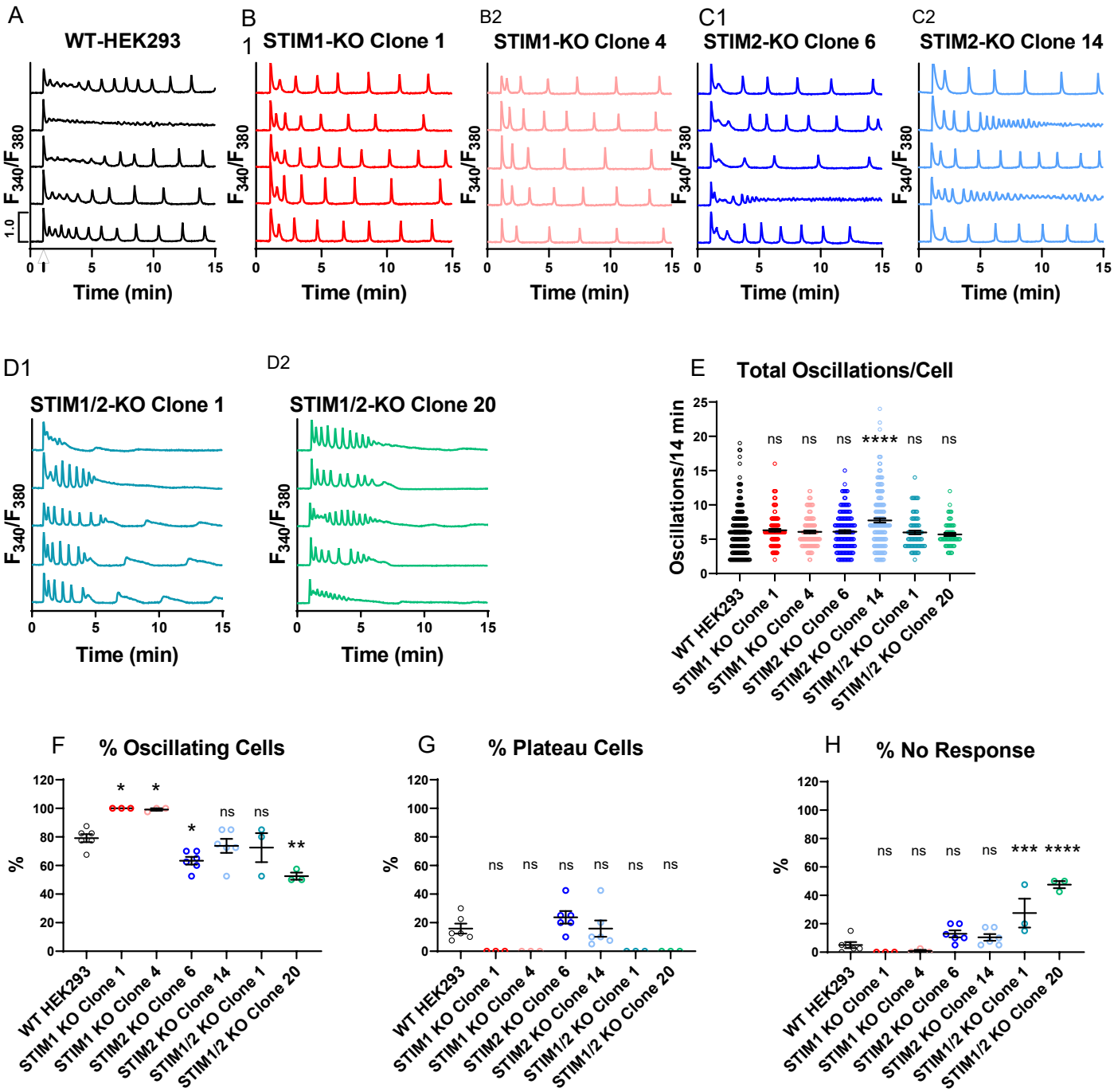


**Supplementary Figure 2. $Ca^{2+}$ oscillations from two independent clones for each of HEK293 STIM1-KO, STIM2-KO, and STIM1/2-KO cells (Related to Figure 1).** (A) WT HEK293 $Ca^{2+}$ traces from 5 representative cells/condition upon stimulation with 10 μM carbachol (CCh) at 1 minute (indicated by arrow in A) in the presence of 2mM external $Ca^{2+}$. Same conditions as in (A) but for (B) STIM1-KO clones# 1 and 4, (C) STIM2-KO clones# 6 and 14, and (D) STIM1/2-KO clones# 1 and 20. (E) Quantification of total oscillations in 14 minutes. From left to right *n* = 189, 120, 119, 150, 175, 86, and 62 individual cells. Oscillation frequency data in (Fig. 1I) is pooled from the two clones presented in (B-D) for each condition. (F) % oscillating cells, (G) % plateau cells, and (H) % non-responding cells for each cell line shown in (A-D). For (F-H) from left to right *n* = 6, 3, 3, 6, 6, 3 and 3 independent experiments. Scatter plots of oscillation frequency data (E) are presented as mean ± SEM and analyzed with the Kruskal-Wallis one-way ANOVA with multiple comparisons to WT HEK293 cells (****p<0.0001; ns, not significant). Scatter plots in (F-H) are presented as mean ± SEM and analyzed with an ordinary one-way ANOVA with multiple comparisons to WT HEK293 cells (*p<0.05; **p<0.01; ***p<0.001; ****p<0.0001; ns, not significant).

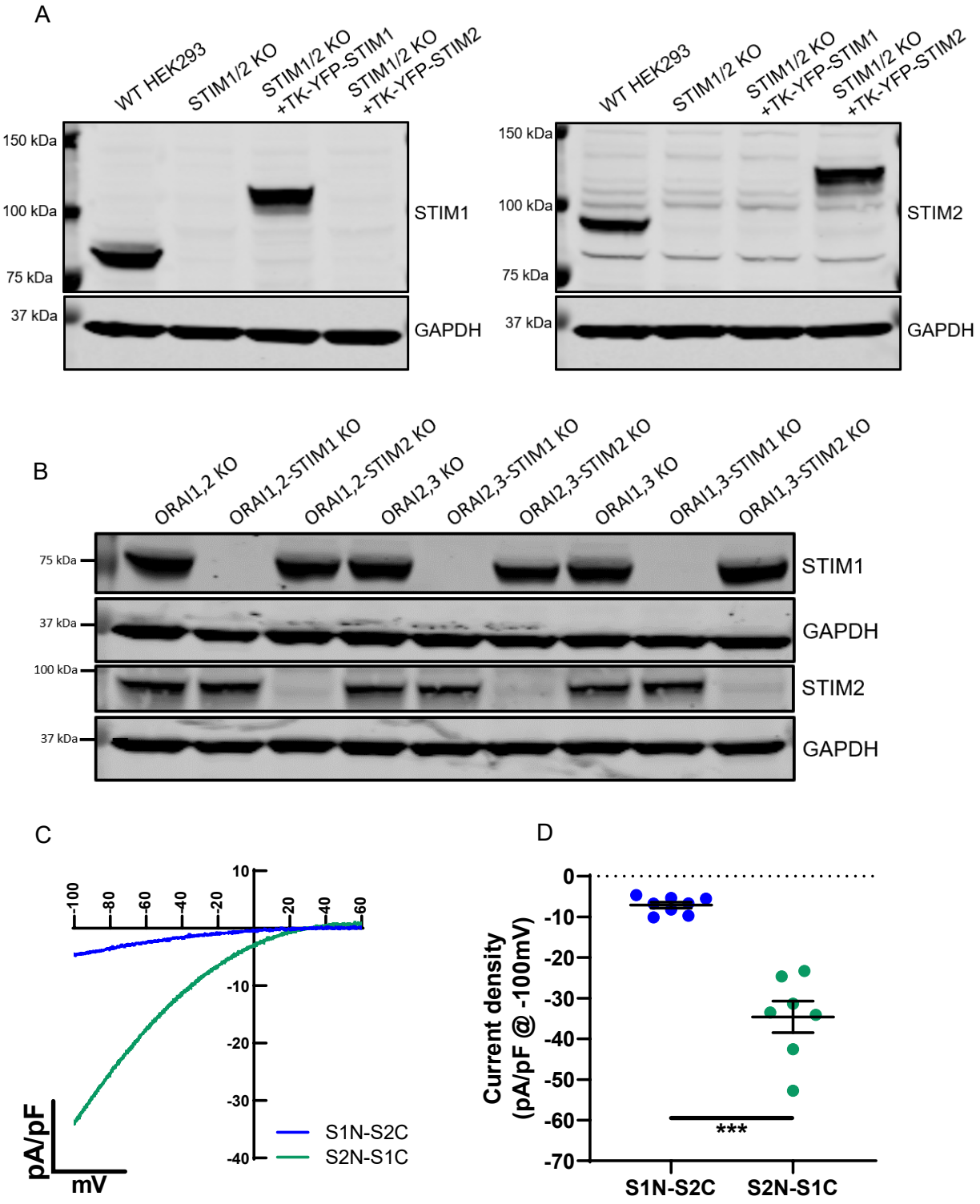


**Supplementary Figure 3. STIM1/2 Western blots in double Orai-STIM knockout cell lines, and CRAC currents mediated by STIM chimeric constructs (Related to Figures 2 and 3).** (A) *Left:* Representative western blots of WT HEK293, STIM1/2-KO cells, and STIM1/2-KO cells rescued with tk-YFP-STIM1 or tk-YFP-STIM2 and probed with primary antibodies against STIM1 and GAPDH. *Right*: Same samples shown in *Left*, but probed with a primary antibody against STIM2. (B) Representative western blots of double Orai-KO/single STIM-KO HEK293 cells probed with primary antibodies against STIM1, STIM2, and GAPDH. (C) Representative I/V curves of whole-cell patch clamp currents in STIM1/2-KO cells expressing CFP-Orai1 with either YFP-S1N-S2C or YFP-S2N-S1C chimeric STIM constructs. In these recordings, store depletion was achieved through dialysis of 20mM BAPTA through the patch pipette. (D) Quantification of peak current density at -100mV from (C). For each condition $n$ = 8 (S1N-S2C + Orai1) and $n$ = 7 (S2N-S1C + Orai1) individual cells. Scatter plot in (D) is presented as mean ± SEM and analyzed with the Mann-Whitney U test (***p<0.001).

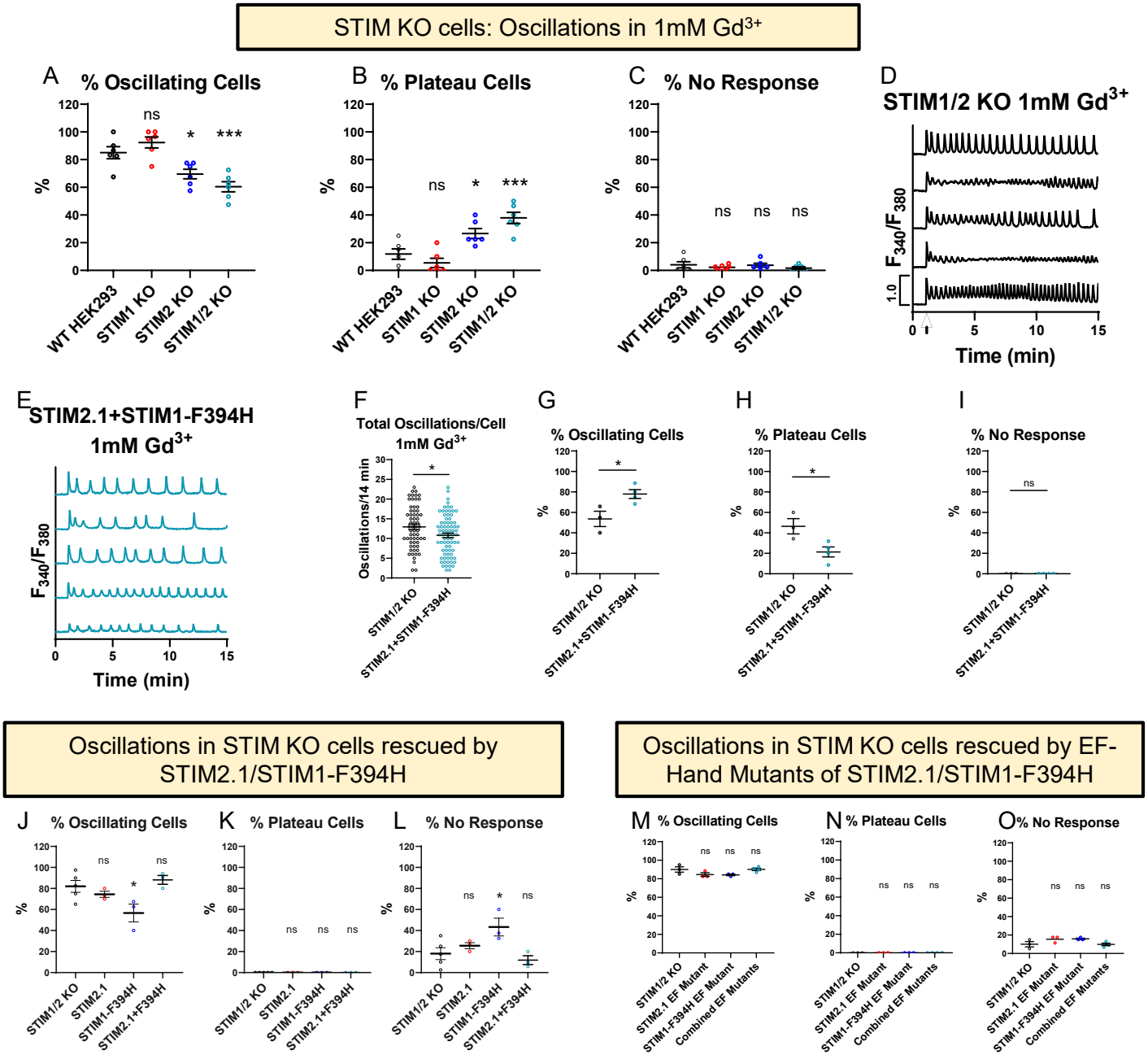


**Supplementary Figure 4. Quantifications of $Ca^{2+}$ signaling events in STIM-KO cells with the lanthanide insulation protocol or rescue with the non-agonist STIM mutants (Related to Figure 4).** Quantification of (A) % oscillating cells, (B) % plateau cells, and (C) % non-responding cells for each cell type shown in (Fig. 4A-D). From left to right *n* = 6, 6, 6, and 6 independent experiments. (D) Representative $Ca^{2+}$ oscillation traces of STIM1/2-KO cells and (E) STIM1/2-KO cells rescued with combined YFP-STIM2.1 + STIM1-F394H-CFP and stimulated with 10 μM carbachol (CCh) at 1 minute (indicated by arrow in D) in the presence of 1mM $Gd^{3+}$ and 2mM external $Ca^{2+}$. (F) Quantification of total oscillations in 14 minutes from (D-E). From left to right *n* = 62 (STIM1/2-KO) and *n* = 77 (STIM2.1+STIM1-F394H) individual cells. (G) % oscillating cells, (H) % plateau cells, and (I) % non-responding cells for each cell type shown in (D-E). For (G-I) from left to right *n* = 3 independent experiments for both conditions. Quantification of (J) % oscillating cells, (K) % plateau cells, and (L) % non-responding cells for each cell line shown in (Fig. 4K-O). From left to right *n* = 5, 3, 3, and 3 independent experiments. Quantification of (M) % oscillating cells, (N) % plateau cells, and (N) % non-responding cells for each cell line shown in (Fig. 4R-V). From left to right *n* = 3, 3, 3, and 4 independent experiments. Scatter plots in (A-C, J-L, M-O) are presented as mean ± SEM and analyzed with an ordinary one-way ANOVA with multiple comparisons to WT HEK293 (A-C) or STIM1/2-KO (J-L, M-O) where (*p<0.05; ***p<0.001; ns, not significant). Scatter plots in (F-I) are presented as mean ± SEM and analyzed with an unpaired Student's t-test (F) or Mann-Whitney U test (*p<0.05; ns, not significant).

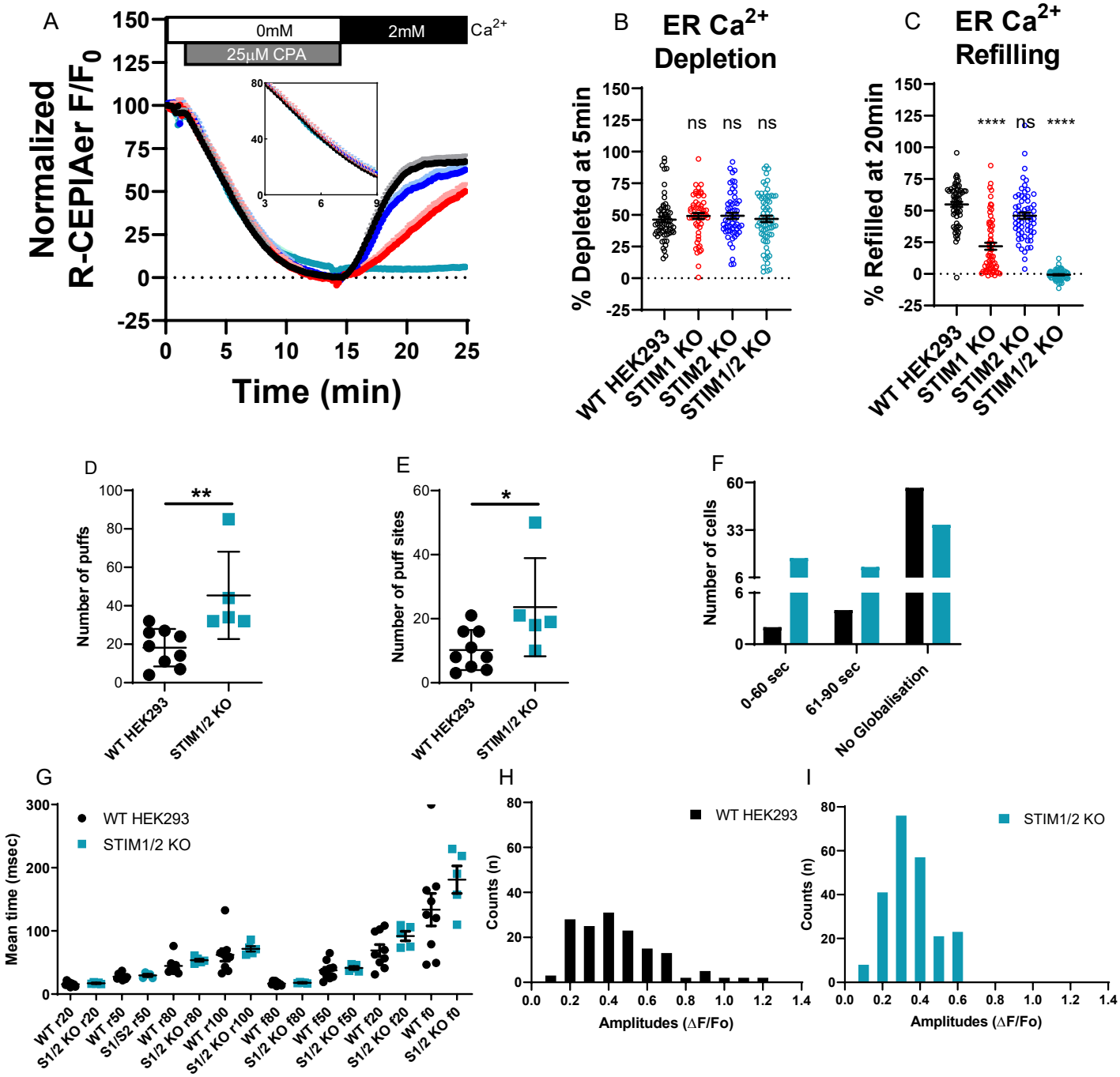


**Supplementary Figure 5. STIM1/STIM2 regulate $IP_3R$-mediated $Ca^{2+}$ puffs in response to carbachol stimulation (Related to Figure 5).** (A) Measurement of ER $Ca^{2+}$ in HEK293 STIM-KO cells using R-CEPIA1*er*. Cells were stimulated with 25µM CPA in a 0mM $Ca^{2+}$ bath solution followed by re-addition of 2mM $Ca^{2+}$ at 15 min (without CPA). Inset shows zoomed in trace from 3-9 min (B) Quantification of ER $Ca^{2+}$ depletion rate in (A) at 5 min after CPA stimulation in 0mM external $Ca^{2+}$. (C) Quantification of ER $Ca^{2+}$ refilling rate in (A) at 20 min after restoration of 2mM external $Ca^{2+}$. From left to right *n* = 63, 56, 57, and 70 individual cells. Scatter plots of ER $Ca^{2+}$ depletion and refilling quantifications are presented as mean ± SEM and analyzed with the Kruskal-Wallis one-way ANOVA with multiple comparisons to WT HEK293 (****p<0.0001; ns, not significant). (D) Number of $Ca^{2+}$ puffs were elicited by addition of 1 µM CCh to WT-HEK293 (n= 9 independent experiments with 63 cells) and STIM1/2-KO cells (n= 5 independent experiments with 65 cells). The number of puffs were significantly higher in STIM1/2-KO (227 in 65 cells) when compared to HEK293 cells (164 in 63 cells). Similarly, (E) The number of puff sites were significantly higher in STIM1/2-KO (118 in 65 cells) when compared to HEK293 cells (92 in 63 cells). (F) Bar graph showing the number of WT-HEK293 and STIM1/2-KO cells in which the calcium signals globalize within 0-60 seconds or 61-90 seconds following CCh perfusion. Also, shown are the number of cells in which the calcium signals do not globalize. (G) Mean rise and decay times for the fluorescence to increase or decrease to 20%, 50%, 80%, 100% of $Ca^{2+}$ puffs evoked by CCh from HEK293 (n=63) and STIM1/2-KO (n=65) cells are plotted. (H, I) Histograms representing the amplitudes distribution of the $Ca^{2+}$ puffs following stimulation with CCh of WT-HEK293 (H) and STIM1/2-KO cells (I). Data presented as mean ± SEM. Statistical significance was determined by student's t-test (unpaired, two-tailed). *p<0.05, **p<0.01 with respect to HEK293. ns, not significant.

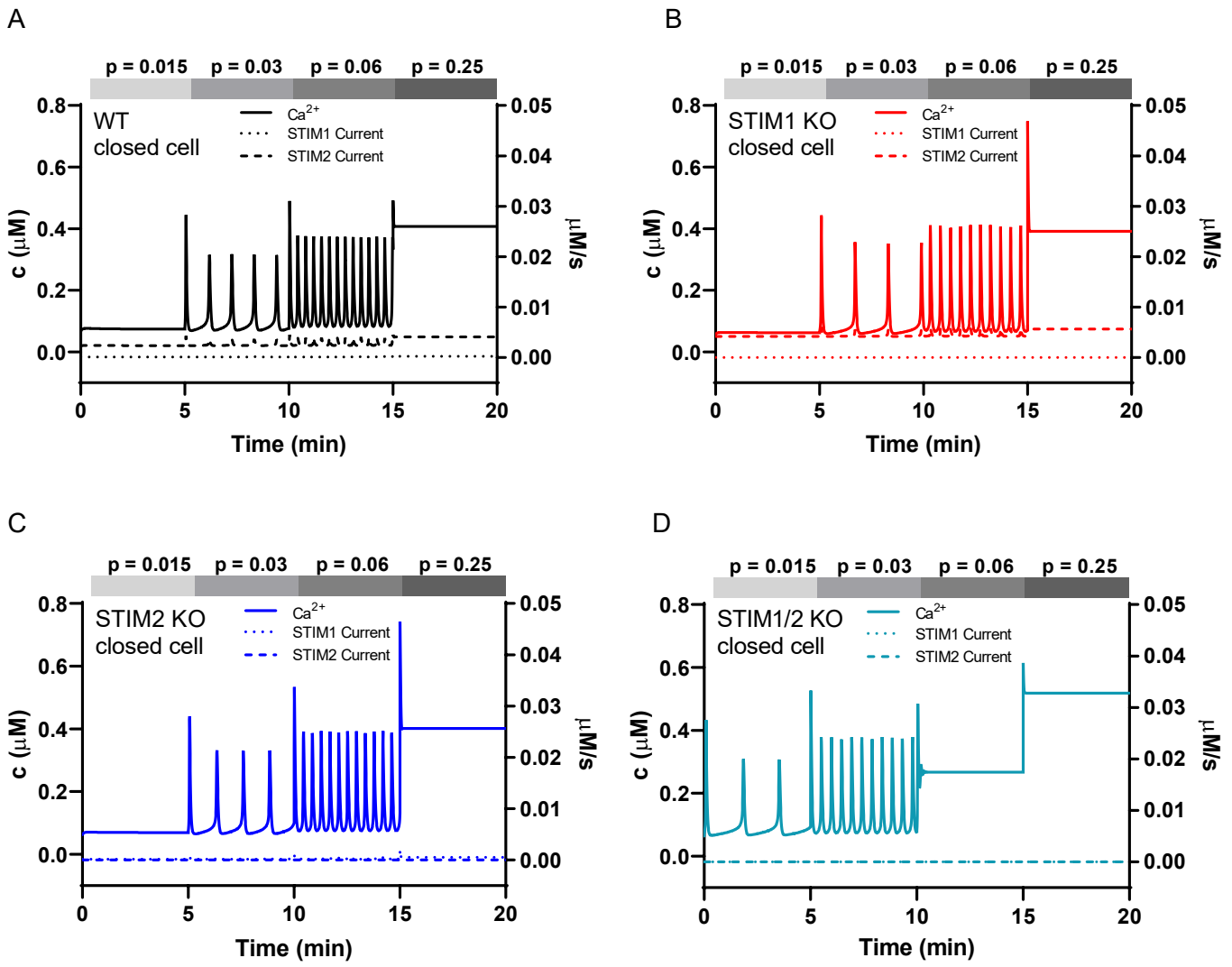


**Supplementary Figure 6. Mathematical model simulations of $Ca^{2+}$ responses to increasing agonist concentrations under the $Gd^{3+}$ insulation protocol in WT and STIM-KO cells (Related to Figure 6).** Responses to four different agonist concentrations ($p$ = 0.015, $p$ = 0.03, $p$ = 0.06, $p$ = 0.25) applied sequentially in that order, each for 5 min. In each panel the solid line is the $Ca^{2+}$ concentration, and is plotted against the left axis, while the dotted and dashed lines are the STIM-mediated currents, and are plotted against the right axis. Panels A-D; $Ca^{2+}$ responses in a closed cell system, mimicking the 1mM $Gd^{3+}$ insulation protocol (i.e., with no membrane influx of extrusion of $Ca^{2+}$) with all three Orai isoforms present. The STIM1/2-KO cell is the most effective oscillator, which results from the model assumption that the $IP_3R$ is inhibited by unactivated STIM. Under this $Gd^{3+}$ insulation protocol (closed cell), the absence of STIM1 (B and D) does not hinder the cell from responding with a raised plateau of $Ca^{2+}$ at high agonist concentrations.

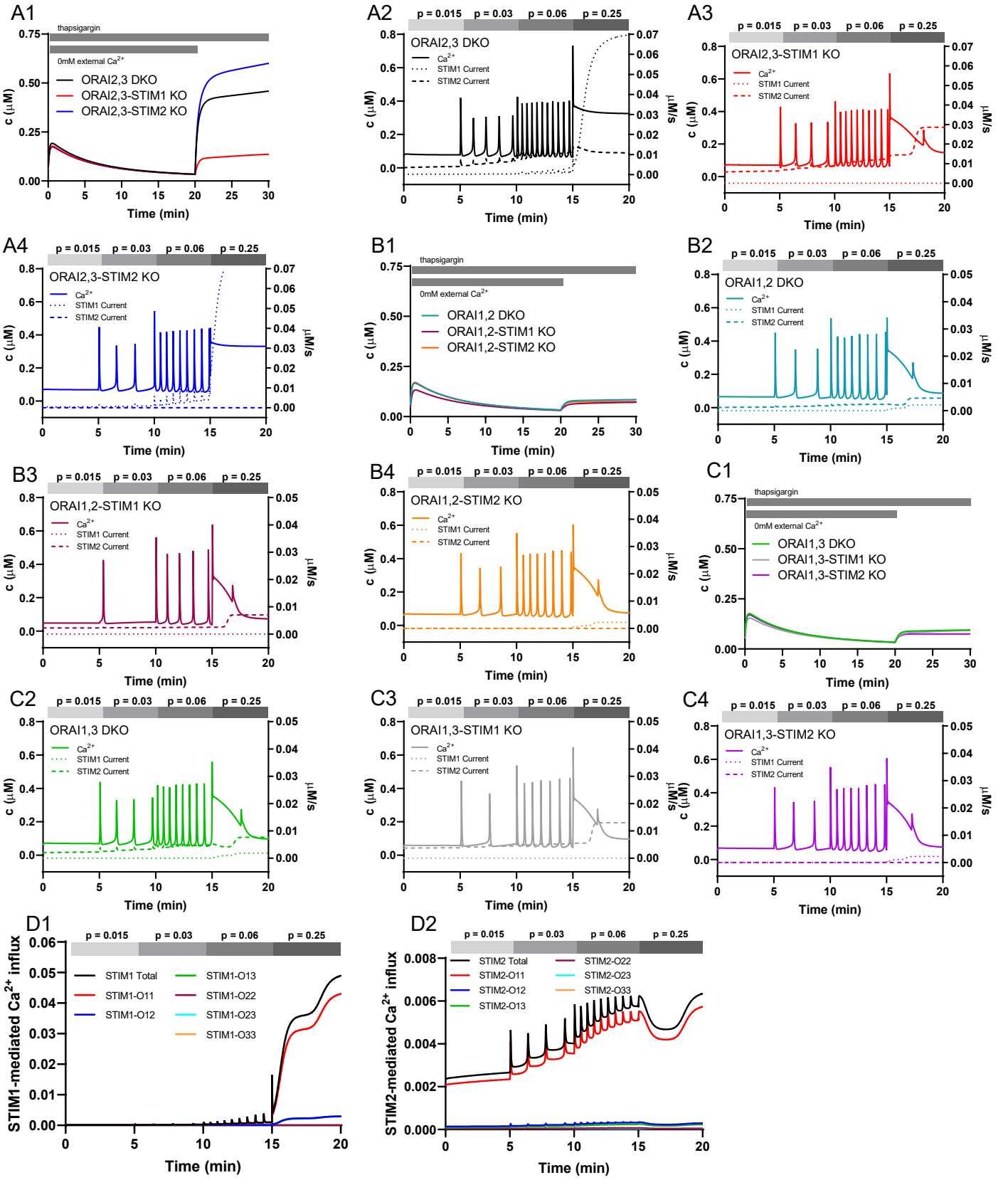


**Supplementary Figure 7. Mathematical model simulations of $Ca^{2+}$ responses to thapsigargin and increasing agonist concentrations in double Orai-KO/single STIM-KO cells (Related to Figure 6).** Responses to thapsigargin (panels A1, B1 and C1) and responses to increasing steps of agonist concentration ($p$ = 0.015, $p$ = 0.03, $p$ = 0.06, $p$ = 0.25) applied sequentially in that order, each for 5 min (other panels). The left panels (A1, A2, A3, A4) are for an Orai2,3-DKO cell, the middle panels (B1, B2, B3, B4) are for an Orai2,3-DKO cell, and the right panels (C1, C2, C3, C4) are for an Orai1,3-DKO cell. For each column of panels, the color coding described in the top panel refers also to the lower panels. These responses reproduce the qualitative features seen in the experimental data and cells are unable to maintain $Ca^{2+}$ plateaus in the absence of STIM1. Simulations of STIM1-mediated (D1) and STIM2-mediated (D2) $Ca^{2+}$ currents in response to increasing concentrations of agonist (denoted by p) in various Oraij,k conditions.